

Institut d'Optique Graduate School

centre for nanoscience and nanotechnology



M2 Internship report

optimization subwavelength nanostructures for hybrid integration of active materials

Author: HE Puyuan

supervisor: Carlos ALONSO-RAMOS

*A thesis submitted in fulfillment of the requirements for
the joint UvA-VU Master of Science degree in Computer Science*

August 18, 2021

Contents

1	Introduction	3
1.1	Taper coupler	3
1.2	Grating coupler	3
2	Subwavelength	3
3	Simulation tools	3
3.1	Lumerical	3
3.2	FDTD method	3
4	Simulation subwavelength	5
4.1	L-shaped fiber grating coupler	5
4.1.1	Simulation setting	5
4.1.2	Result analysis	6
4.2	Grating coupler with subwavelength structure arranged in matrix	8
4.2.1	Building simulation structure	9
4.2.2	Normalized structural parameters	10
4.2.3	Apodization optimization	11
5	Create structures in Graphic Data System (GDS)	13
5.1	GDS introduction	13
5.2	GDSPY in Python	13
6	Measurement	13

1 Introduction

this is the introduction of optical coupler and fiber-chip grating coupler.

$$a = 1$$
$$b = c + \frac{a}{b}$$

1.1 Taper coupler

1.2 Grating coupler

2 Subwavelength

3 Simulation tools

3.1 Lumerical

3.2 FDTD method

Finite Difference Time Domain (FDTD) was proposed by Chinese-American Yee in 1966. It is a method of solving Maxwell equation. Its core idea is to discretize the solution space into a rectangular parallelepiped network structure in Cartesian coordinates. Each point is assigned an electric field and a magnetic field. As time changes, each point alternately updates the electric field and magnetic field in the form of leaping. In essence, FDTD is the most primitive and perfect simulation of electromagnetic field problems, and has a very wide range of applicability. Below I'll do a brief introduction of FDTD solutions.

Assuming that the research space is passive, and the media parameters a , b , and c do not change with time, in the rectangular coordinate system (x, y, z) , Maxwell's equations can be written as six scalar equations.

$$\begin{aligned}\frac{\partial H_z}{\partial y} - \frac{\partial H_y}{\partial z} &= (\sigma + \varepsilon \frac{\partial}{\partial t}) E_x & \frac{\partial E_y}{\partial z} - \frac{\partial E_z}{\partial y} &= (S + \mu \frac{\partial}{\partial t}) H_x \\ \frac{\partial H_x}{\partial z} - \frac{\partial H_z}{\partial x} &= (\sigma + \varepsilon \frac{\partial}{\partial t}) E_y & \frac{\partial E_z}{\partial x} - \frac{\partial E_x}{\partial z} &= (S + \mu \frac{\partial}{\partial t}) H_y \\ \frac{\partial H_y}{\partial x} - \frac{\partial H_x}{\partial y} &= (\sigma + \varepsilon \frac{\partial}{\partial t}) E_z & \frac{\partial E_x}{\partial y} - \frac{\partial E_y}{\partial x} &= (S + \mu \frac{\partial}{\partial t}) H_z\end{aligned}$$

On this basis, dividing the space into many grid cells along the three coordinate axes, using Δx , Δy and Δz to respectively indicate the length of the cells along the three axes and Δt to indicate the time increment. The coordinates (x, y, z) of the grid origin can be written as

$$(i, j, k) = (i\Delta x, j\Delta y, k\Delta z)$$

Any space and time function can be expressed as

$$F^n(i, j, k) = F(i\Delta x, j\Delta y, k\Delta z, n\Delta t)$$

Here i , j , k and n are integers.

Secondly, the center-only finite differential formula is used to express the partial derivative of the function with respect to space and time. This differential formula has second-order accuracy, and its expression is

$$\frac{\partial F^n(i, j, k)}{\partial x} = \frac{F^n(i + 1/2, j, k) - F^n(i - 1/2, j, k)}{\Delta x} + \mathcal{O}(\Delta x^2)$$

$$\frac{\partial F^n(i, j, k)}{\partial t} = \frac{F^{n+1/2}(i, j, k) - F^{n-1/2}(i, j, k)}{\Delta t} + \mathcal{O}(\Delta t^2)$$

In order to achieve the differential calculation of the space coordinates, and taking into account the orthogonal relationship of the electromagnetic field in space, the positions of the six field components on the basic network unit are shown in the following figure:

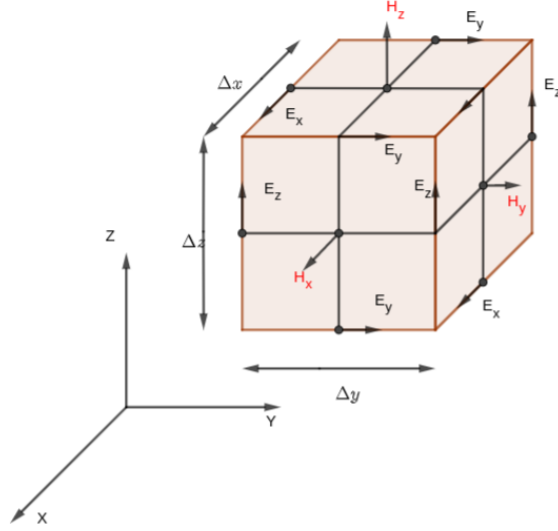


Figure 1: Field distribution on the basic space unit

In addition, it should be considered that E and H have a half time step change in time. Therefore, by introducing the differential expression above, the scalar Maxwell's equations can also be rewritten into a differential form.

The solving steps of the FDTD numerical solution can be summarized as follows:

1. Expand Maxwell's curl equation in the time domain into its coordinate components. The central finite difference is used to replace the differentiation of each component field with respect to space and time, and the basic equation of FDTD is obtained.
2. Determine the basic unit size Δx , Δy and Δz of the spatial grid.
3. Choose the time step Δt . The choice of Δt should ensure the stability of the numerical calculation, and its discriminant is

$$\Delta t \leq \frac{1}{c_{max}} \frac{1}{\sqrt{\frac{1}{\Delta x^2} + \frac{1}{\Delta y^2} + \frac{1}{\Delta z^2}}}$$

where c_{max} is the maximum wave number of the mode that exists in the target space. In generally we choose $\Delta t = \Lambda/(2c_{max})$, Λ is the minimum value among Δx , Δy and Δz .

4. Determine the size of the target space and set the absorbing boundary conditions along the outer surface of the grid space. At the same time select and set the excitation source.

5. Determine the total number of time steps for the calculation and estimate the amount of storage for the calculation. When the storage capacity of the calculation is large, the calculation is generally performed on the server.

4 Simulation subwavelength

Simulation is one of the main contents of my internship research. By constructing the corresponding theoretical model on the computer, with the help of Lumerical and other software, we can easily obtain the characteristic parameters of the subwavelength structure or the grating structure. This not only provides me with high-precision theoretical results, but also saves my design time to a large extent. On this basis, I can also easily use sweep and other functions provided by the Lumerical to continuously optimize the simulation structure to obtain more suitable design parameters. In this part, I mainly simulated and optimized the three structures: L-shaped fiber-chip coupler, a symmetrical SOI waveguide with gradually changing width and Grating coupler with subwavelength structure arranged in matrix.

4.1 L-shaped fiber grating coupler

Firstly, I will study the L-shaped fiber-chip coupler, optimizing the related parameters and, at the same time, gradually mastering the use of Lumerical FDTD-solutions. It's worth mentioning, by adding a subwavelength structure at the beginning, the L-shaped fiber-chip coupler can provide a high coupler efficiency and a remarkably high grating directionality with a simplified fabrication process, compared with blazed gratings.

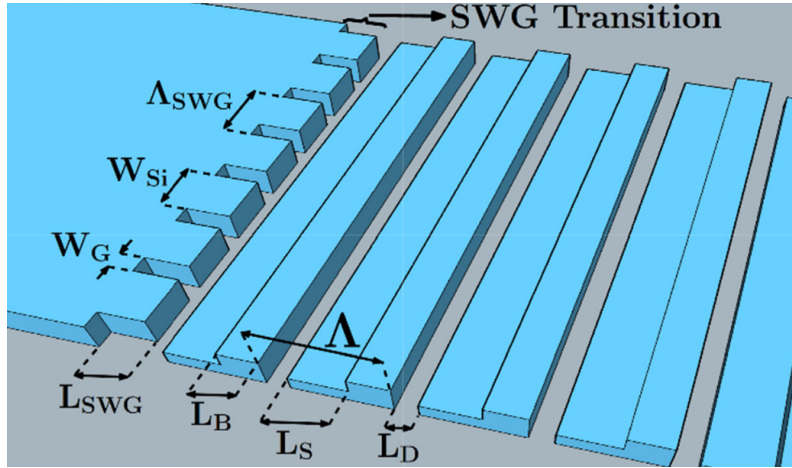


Figure 2: L-shaped fiber-chip coupler

The figure 1 above shows the 3D structure of the L-shaped fiber-chip coupler. The following simulation work based on this structure. The main purpose of my work for this structure is trying to reproduce the result mentioned in an article, to fulfill the high coupler efficiency and ultra direction.

4.1.1 Simulation setting

For the convenience of description, I assume the direction in which the L-shape structure cycle repeats as x direction, the direction in which the subwavelength structure cycle repeats as z direction and the left as y directions.

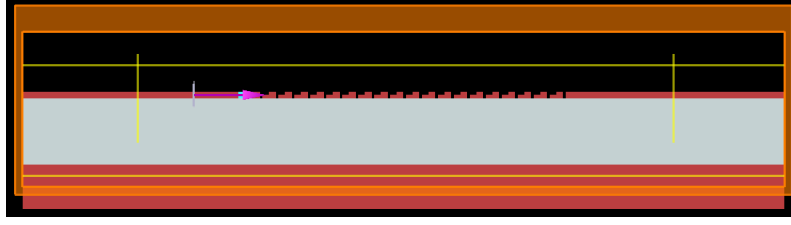


Figure 3: simulation model XY view

Refer to the parameter setting in figure 1, the grating coupler is implemented on a 300-nm-thick Si layer in 300 nm SOI wafer, relying on standard full (300 nm) and shallow (150 nm) etch steps. Here I set the length of the subwavelength part is $L_{SWG} = 255nm$. The subwavelength period $\Lambda_{SWG} = 400nm$ comprises the width of silicon $W_{si} = 300nm$ and the width of gap $W_{gap} = 100nm$. The grating period $\Lambda = 720nm$ comprises the deep- and shallow-etch trenches of lengths $L_D = 120nm$ and $L_S = 290nm$, respectively, and unetched Si block of length $L_B = 310nm$. The structure is optimized for transverse electrical (TE) mode, which means the polarization direction of the incident light is along the z direction. In the simulation, I create the FDTD for the whole input part, grating part and output part, setting the boundary condition as PML. Also I add 4 monitors. The monitor at the top of the grating is arranged to measure the energy of the diffracted light, which will be used to couple to a specific mode to calculate the coupler efficiency. And the monitors at the right and left are arranged to measure the transmitted energy and reflected energy.

4.1.2 Result analysis

Through the setting mentioned above, I can first directly get the energy received by the top monitor, left monitor and right monitor. One thing needs to pay attention that all the operation is in the C-band near $1.55 \mu m$ (I take the wavelength from $1.5 \mu m$ to $1.6 \mu m$).

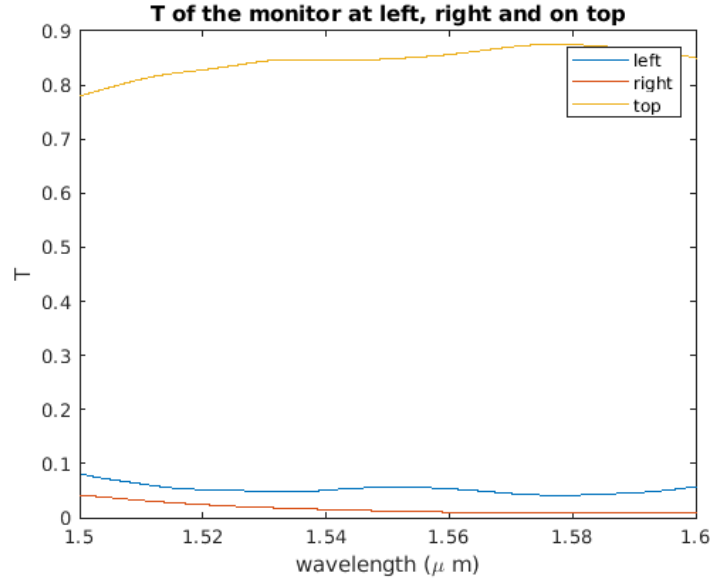


Figure 4: simulation model XY view

From the figure above we can see most of the energy is received by the monitor on the top. In fact it's a good sign, which means the grating coupler succeed in diffracting most of energy to a

different plane (out of the waveguide transmission plane). This lays a solid foundation for excellent coupling efficiency in the future.

After knowing the information above, I tend to study the coupler proceed. Without affecting the generality, we can suppose to use this L-shaped grating coupler to couple the light on a chip to an optical fiber in the free space. Then the position (the angle of the fiber relative to the chip) and mode matching of the fiber will be critical to the coupling efficiency. This is because the proper position can ensure optical fiber to receive more energy of the diffracted light. The mode matching or not, on the other hand, determines whether the energy received can successfully enter the optical fiber for stable transmission. Here I consider the wavelength is $1.55 \mu\text{m}$ and assume the light pulse transmitted in the optical fiber is a Gaussian pulse.

$$Gaussian_{norm,angle} = \frac{1}{\sqrt{I}} \exp\left(\frac{-(x - x_0)^2}{\sigma^2}\right) * \exp\left(\frac{2i\pi n_{cladding}}{\lambda}\right) * \sin(\alpha)$$

The $Gaussian_{norm,angle}$ present the normalized Gaussian pulse, where the I is the optical intensity, λ is the wavelength. From the formula above it's obvious to see that the position of the fiber will determine the value of x_0 and angle α . On this basis, I can express the coupling efficiency as the product of Overlap and the amount of received light.

$$Coupling\ efficiency = Overlap * T = \left| \int E_{z,norm} * (Gaussian_{norm,angle})^* dx \right| * T$$

where the $E_{z,norm}$ is the electric filed of the light incident on the optical fiber, the T is the energy received by the top monitor (The T of the top monitor in figure 3).

Based on the above analysis, we can first consider the directionality of the L-shaped fiber-chip coupler. Through Lumerical FDTD-solutions, I can easily get the result of *Overlap* with the change of angle and x_0 .

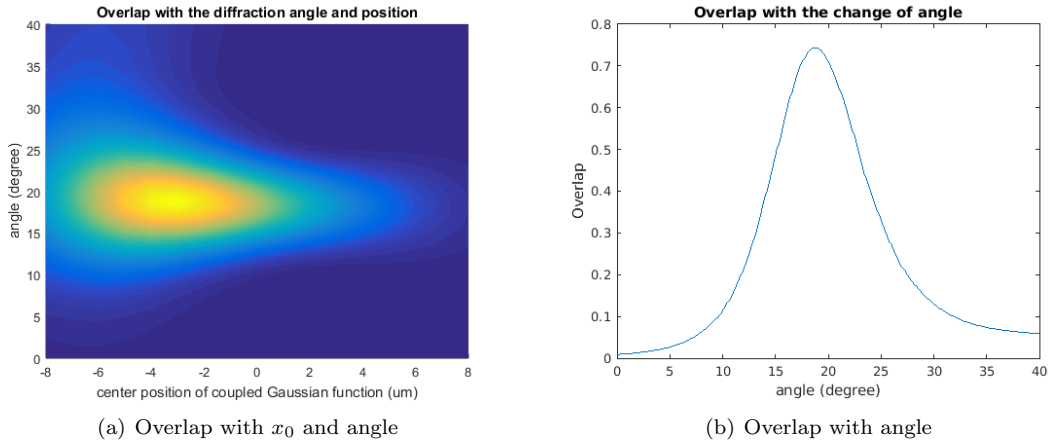


Figure 5: Overlap

Here the figure present the change of Overlap with the change of angle and x_0 . Also the figure 4-b directly present the relationship between angle and Overlap. It's worth mentioning when angle equals to 18.8° the Overlap achieves its maximum value 0.7437. This is ideal for my expectations. It provides the possibility for higher coupling efficiency. Then I take the best angle for overlap to calculate the coupling efficiency.

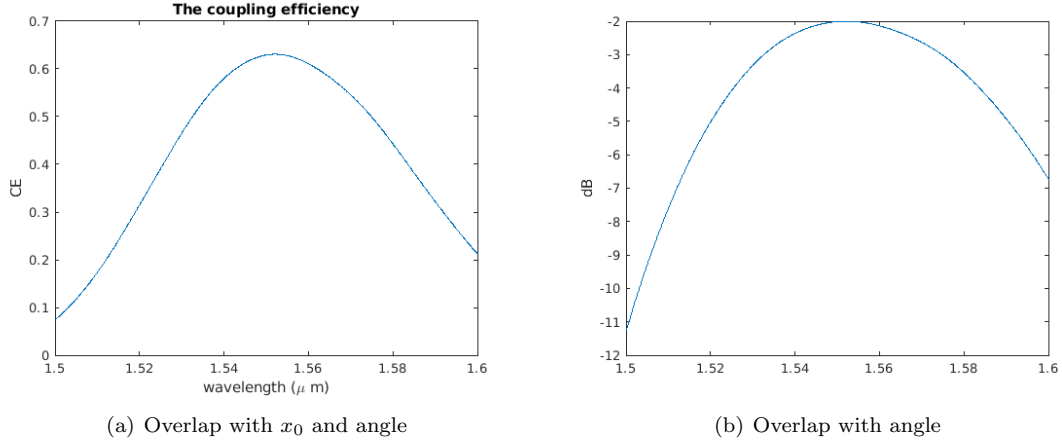


Figure 6: Coupling efficiency

Here a simulation peak coupling efficiency is 0.6307 (-2.0015 dB) taken at 1552.1 nm. The -3 dB bandwidth is 42 nm.

4.2 Grating coupler with subwavelength structure arranged in matrix

In the end instead of adjusting the shallow etch depth of grating grooves to engineer the grating strength like what I've explained in the L-shaped fiber-chip coupler part, here using a fully etched SWG structure as was first proposed by Halir et al, which allows efficient grating apodization and simplifying fabrication.

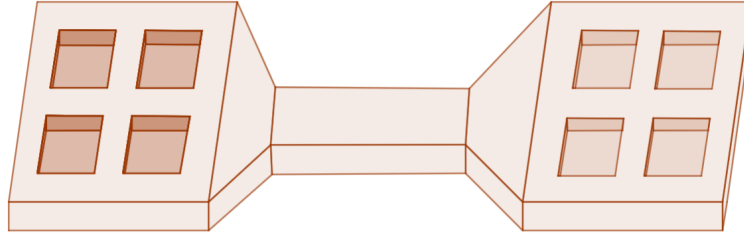


Figure 7: The grating structure

This structure should includes grating coupler part, a taper, a waveguide, a taper and a grating decoupler part. Below is the Decoupled two-dimensional models, illustrated in fig. a) and fig. b), are used in the yz-plane and xz-plane to model the diffractive grating and the SWG structure.

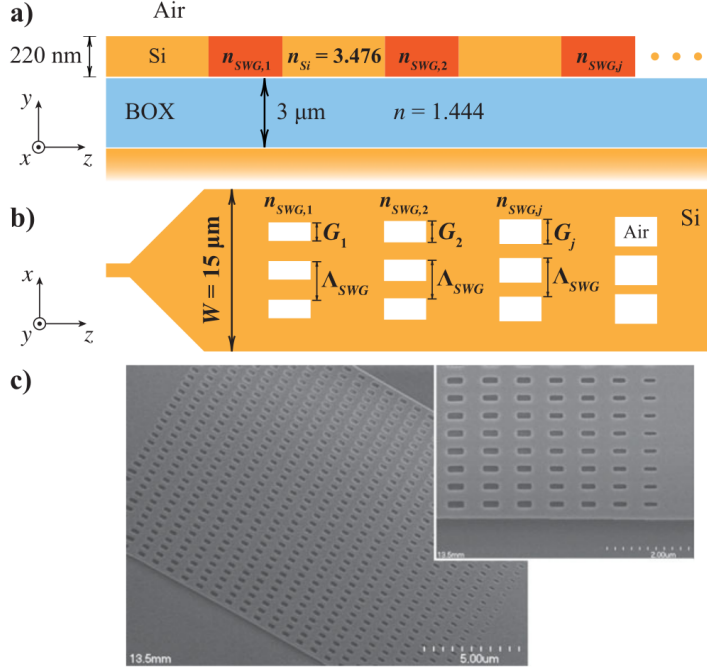


Figure 8: (a) Two-dimensional vertical cross-section schematic of SWG coupler. (b) Two-dimensional in-plane schematic of SWG coupler. (c) Scanning electron microscopy image of fabricated continuously apodized coupler. Inset: detailed view.

The SWG is a periodic structure implemented by interleaving two constituent materials, here silicon and air, with refractive indices $n_{Si} = 3.476$ and $n_{air} = 1$. Here I assume the light transmits in z direction and then coupled to a optical fiber above the coupler by the grating structure. The width of the SWG structure should be $W = 15 \mu m$ and the length of the whole grating part should be $L = 40 \mu m$. Then I note the width (in x direction) of the air gap and silicon gap as W_{air} and W_{Si} , the length (in z direction) of the air gap and silicon gap as L_{air} and L_{Si} .

4.2.1 Building simulation structure

According to the previous analysis, it can be known that this kind of long periodic structure (which can form multiple resonant cavities) is almost impossible to run 3 dimensional simulation in Lumerical. Therefore, it is very important to simplify the target structure to achieve two-dimensional simulation, which means the structure should be changed to be invariant in the x direction. Therefore, in the z direction, for the periodic part of the structure that contains air, we can equate it to a substance with a refractive index of n_{SWG} (as in figure11 (a)). Obviously, the value of n_{SWG} should be between n_{air} and n_{Si} , and is determined by the duty cycle in the x direction. From this perspective, in the simulation, n_{SWG} can be assigned directly, and when optimized to the optimal situation (to get the best coupling efficiency), the values of n_{air} and n_{Si} are determined according to the corresponding n_{SWG} value. This not only simplifies the simulation process but also greatly saves simulation time. Below is the model I used in the Lumerical FDTD-solutions.

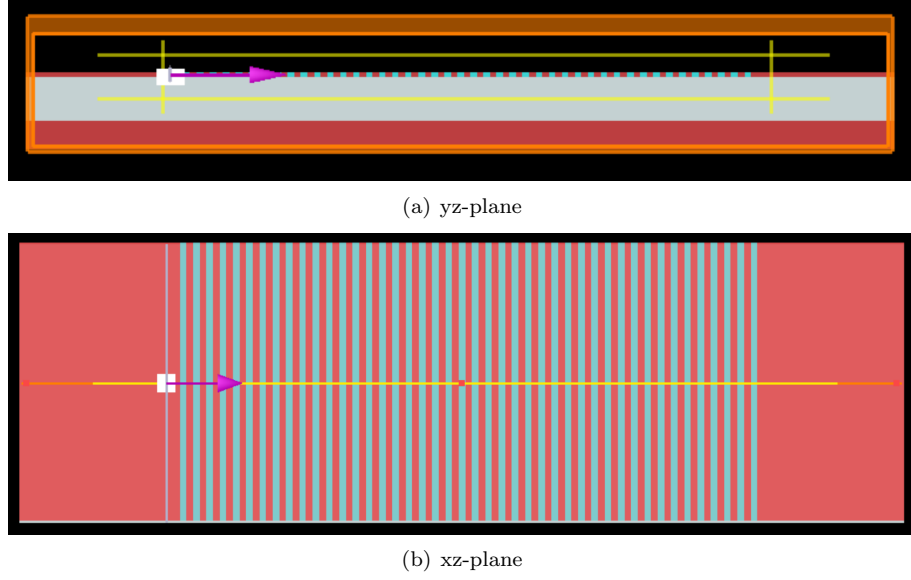


Figure 9: The simulation model of the decoupler grating part

The following is optimized for the above structure, mainly adjusting n_{SWG} , L_{Si} and L_{air} , hoping to obtain the best coupling efficiency. The target wavelength is $1.55 \mu m$.

4.2.2 Normalized structural parameters

Here I firstly consider normalized structural parameters, the simplest situation, which means that I keep all n_{SWG} the same value in the z direction. Considering the n_{SWG} should be bigger than the n_{air} and smaller than the n_{Si} , I take $n_{SWG} = 2.2, 2.3, 2.4, \dots, 2.8$. Then for the length of the silicon and air, I keep them change in the range of $0.21 \mu m$ to $0.45 \mu m$, with the step equal to $0.03 \mu m$. After that, I calculated every combination of n_{SWG} , L_{si} , and L_{gap} in Lumerical, and checked the light energy received by each monitor (top, left, right).

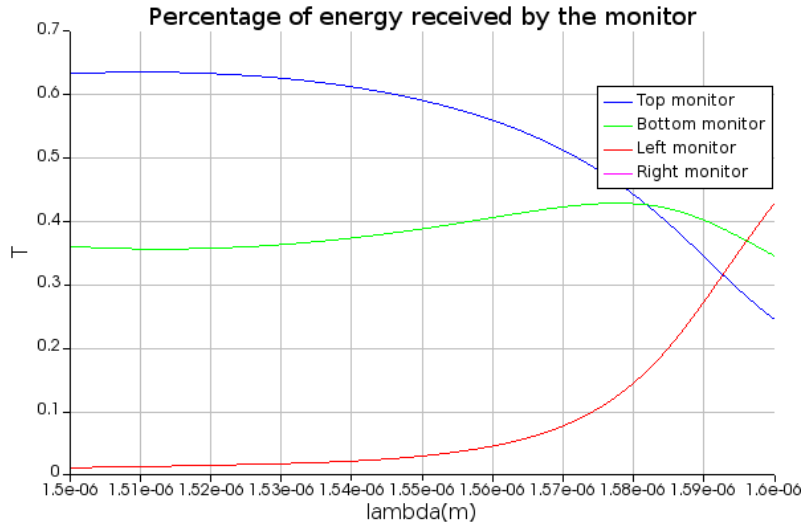


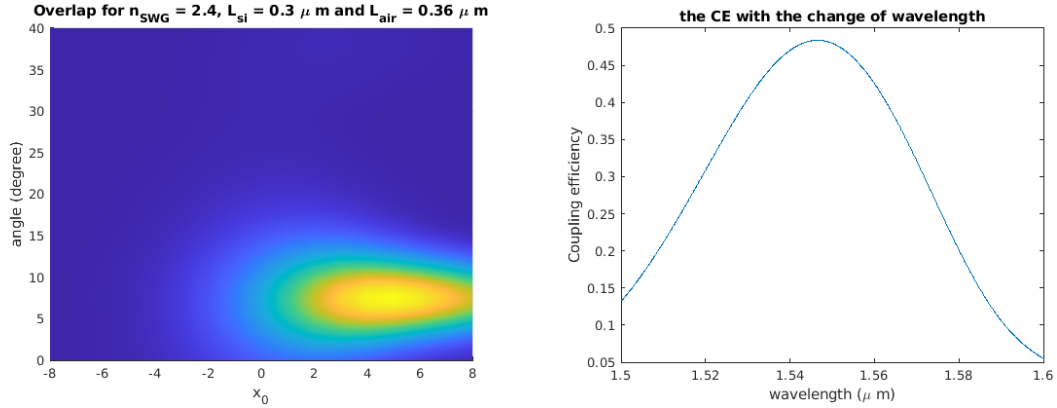
Figure 10: $n_{SWG} = 2.4$, $L_{si} = 0.3 \mu m$ and $L_{air} = 0.36 \mu m$

Similar to the content shown in 4.1, suppose an optical fiber is located above grating, assuming the transmission mode in the optical fiber to Gaussian distribution, then calculate the overlap and coupling efficiency. Here I note the value of n_{SWG} , L_{Si} and L_{air} for the maximum overlap and maximum coupling efficiency. Also noting the coupling angle for the two situations.

Table 1: Best combination of n_{SWG} , L_{Si} and L_{air} for normalized structure

target	target value	angle (degree)	n_{SWG}	$L_{Si}(\mu m)$	$L_{air}(\mu m)$
maximize CE	0.4796	7.5	2.4	0.30	0.36
maximize OL	0.8256	0.9	2.4	0.27	0.36

Below is the corresponding result of Overlap and Coupling efficiency.



(a) Overlap of the best combination of n_{SWG} , L_{Si} and L_{air} maximizing CE (b) The coupling efficiency of best x_0 and $angle$ to maximize Overlap at left

Figure 11: The simulation model of the decoupler grating part

4.2.3 Apodization optimization

Above I've achieved an around -3 dB coupling efficiency. However, there is still a lot of room for optimization. In mathematics, the rearrangement inequality tells how to find the maximum value for a product sum. For every choice of real numbers

$$x_1 \leq x_2 \leq \dots \leq x_n \text{ and } y_1 \leq y_2 \leq \dots \leq y_n ,$$

and every permutation

$$x_{\sigma(1)}, x_{\sigma(2)}, \dots, x_{\sigma(n)} \text{ of } x_1, x_2, \dots, x_n ,$$

the rearrangement inequality states that

$$x_n y_1 + x_{n-1} y_2 + \dots + x_1 y_n \leq x_{\sigma(1)} y_1 + x_{\sigma(2)} y_2 + \dots + x_{\sigma(n)} y_n \leq x_1 y_1 + x_2 y_2 + \dots + x_n y_n .$$

Then we review the formula for calculating coupling efficiency

$$Coupling\ efficiency = Overlap * T = \left| \int E_{z,norm} * (Gaussian_{norm,angle})^* dx \right| * T$$

Through comparison, it can be found that in order to make the value of coupling efficiency as large as possible, it is necessary to ensure that the distribution of E_z and *Gaussian function* satisfies the nature of the rearrangement inequality. In other words, the distribution of the E_z is expected to be similar to Gaussian distribution. However, the previous normalization parameters make the overall structure appear consistent. Therefore, for the monitor located on grating, the received light intensity gradually decreases in the propagation direction. That is, E_z decreases monotonously. This obviously does not correspond to the previous analysis. Therefore, you can consider changing the structural parameters of the first few cycles of grating to make it less "perfect". So that E_z has a gradual increase in the propagation direction first, and then gradually decreases. Therefore, the distribution of E_z is similar to the Gaussian distribution, and theoretically, a better coupling efficiency can be obtained.

Based on the above ideas, I divided grating into two parts along the light propagation direction. The former part contains NA cycles, and the latter part is the remaining part of the grating. At this time, keep the parameters (n_{SWG} , L_{si} and L_{air}) of the latter part the same as the previous optimal normalized parameters. For the previous NA cycles, when NA takes a different value, look for different combination of n_{SWG} , L_{si} and L_{air} again to find the maximum coupling efficiency and its corresponding combination. Here I take $NA = 2, 3, 4, 5, 6, 7$ to do the simulation. The range of n_{SWG} , L_{si} and L_{air} is also the same as before.

Table 2: Apodization optimization

NA	target	target value	n_{SWG}	$L_{si}(\mu m)$	$L_{air}(\mu m)$
2	max CE	0.5141	2.7	0.27	0.36
3	max CE	0.5201	2.7	0.3	0.33
4	max CE	0.5253	2.7	0.3	0.33
5	max CE	0.5309	2.8	0.3	0.33
6	max CE	0.5287	2.8	0.3	0.3
7	max CE	0.5310	2.8	0.3	0.3

From the above results, it can be seen that the coupling efficiency after optimization has improved slightly, but it is difficult to find a trend from it. At this time, there are only three cases for the corresponding combination of n_{SWG} , L_{si} and L_{air} , corresponding to $NA = 2$, $NA = 3, 4, 5$, $NA = 6, 7$. The following uses the values of n_{SWG} , L_{si} and L_{air} corresponding to these three sets of data to record the changes in coupling efficiency by changing the value of NA.

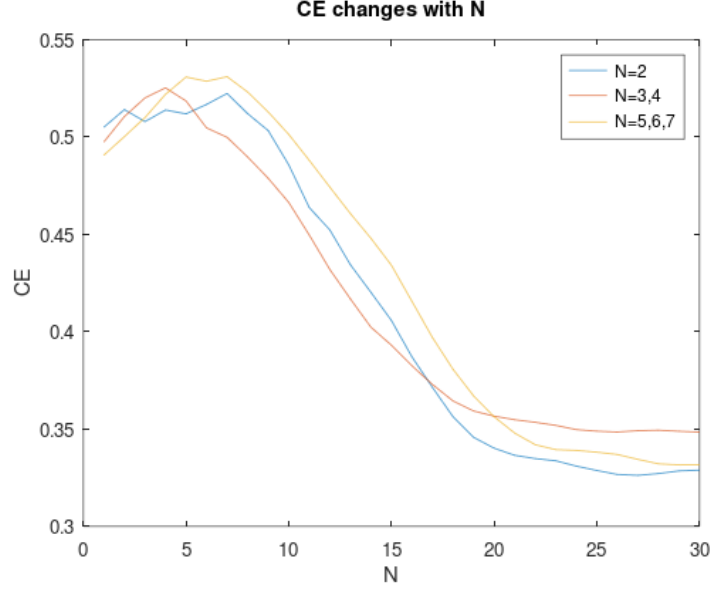


Figure 12: $n_{SWG} = 2.4$, $L_{si} = 0.3\mu m$ and $L_{air} = 0.36\mu m$

Observing the above results, it can be found that the coupling efficiency has been improved after the preliminary optimization, but the improvement is not very ideal. The maximum value of coupling efficiency, which is often obtained between $NA = 4$ and $NA = 8$, is always smaller than 0.54.

5 Create structures in Graphic Data System (GDS)

5.1 GDS introduction

5.2 GDSPY in Python

6 Measurement

References

- [1] asdad